Mechanically triggered heterolytic unzipping of a low-ceiling-temperature polymer

Charles E. Diesendruck[1,2], Gregory I. Peterson[4], Heather J. Kulik[5†], Joshua A. Kaitz[1], Brendan D. Mar[5], Preston A. May[1,2], Scott R. White[2,3], Todd J. Martínez[5,6], Andrew J. Boydston[4] and Jeffrey S. Moore[1,2]*

Biological systems rely on recyclable materials resources such as amino acids, carbohydrates and nucleic acids. When biomaterials are damaged as a result of aging or stress, tissues undergo repair by a depolymerization–repolymerization sequence of remodelling. Integration of this concept into synthetic materials systems may lead to devices with extended lifetimes. Here, we show that a metastable polymer, end-capped poly(o-phthalaldehyde), undergoes mechanically initiated depolymerization to revert the material to monomers. Trapping experiments and steered molecular dynamics simulations are consistent with a heterolytic scission mechanism. The obtained monomer was repolymerized by a chemical initiator, effectively completing a depolymerization–repolymerization cycle. By emulating remodelling of biomaterials, this model system suggests the possibility of smart materials where aging or mechanical damage triggers depolymerization, and orthogonal conditions regenerate the polymer when and where necessary.

M aterials systems with reusable building blocks are attractive for autonomous adaptive structures that have the ability to remodel themselves in response to environmental conditions, including damage or degradation. A familiar example of reusable resources found in nature is the recycling of monomeric building blocks for polymers composed of amino acids[1,2], carbohydrates[1,3] and nucleic acids[1,4]. For synthetic materials, remodelling has the potential to extend device lifetimes through the removal and replacement of defective regions or by restructuring parts to meet their changing mechanical environment. One approach to such adaptive polymeric materials involves mechanically triggered depolymerization followed by mass transfer of the resulting monomer to its newly needed location and subsequent repolymerization. However, mechanochemical bond scission has an inherent limiting molecular weight, below which mechanochemical energy is not accumulated to a degree sufficient to break a covalent bond[5,6]. To overcome this limitation there are two possible solutions: a switchable monomer–polymer equilibrium (which produces large amounts of oligomers) or metastable polymers in which a mechanical event activates complete depolymerization[7–9]. Interestingly, bone tissue, one of the strongest materials in living organisms, is a metastable composite under biological conditions[10]. Both the morphology and properties of bone are dynamic and driven by their mechanical environment, as a consequence of continuous remodelling[11–13].

Above their ceiling temperature T_c, end-capped polymers are potential candidates for mimicking this material-recycling behaviour, with mechanical damage causing reversion to monomers. Below T_c, a chemical initiator drives chain growth. Here, we show that polymer-to-monomer unzipping of a low-T_c poly(o-phthalaldehyde) (PPA)[14,15] can be triggered by force-induced chain scission[5,16–18]. The resulting monomer is subsequently repolymerized under suitable conditions to complete one cycle of use. The

results demonstrate the essential steps for the realization of mechanically induced autonomic remodelling for adaptive and sustainable materials systems.
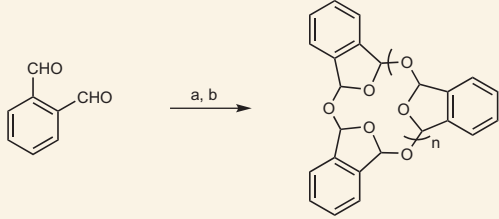
Results and discussion

Preparation and testing of polymers. The molecular weight dependence of the chain scission of polymers in elongational flow fields has been well studied[6]. For polystyrene subjected to ultrasonication, the molecular weight threshold for chain scission is typically around 30 kDa (ref. 16). For our initial studies, we therefore used cationic polymerization to produce cyclic PPA with molecular weights well above the limiting molecular weight (Table 1)[19]. As a reference polymer, we synthesized linear poly(methyl acrylate) (PMA) of comparable molecular weight using controlled radical polymerization[20].

Sonication was used to study the mechanochemical scission[5,6] of the polymers described in Table 1. The polymers were dissolved in THF to a concentration where no chain entanglement is expected (1 mg ml^{-1}), and pulsed ultrasound (0.5 s on, 1.0 s off, 8.7 W cm^{-2}) was applied under argon at −15 °C. Figure 1a–c presents gel-permeation chromatograms of aliquots removed from the Suslick cell during the sonication experiment.

The expected decrease in molecular weight was observed for both PPA_{90}^C and PMA_{103}^L. In great contrast to PMA_{103}^L, the integrated PPA_{90}^C peak area decreases during the experiment, indicating a decline in polymer concentration with sonication time (Fig. 1a). Such a decrease is consistent with mechanochemical scission followed by rapid unzipping to monomer. Moreover, a gradual increase of a new peak close to the column dead-volume is also observed in this case, presumably resulting from an increase in monomer concentration. The gel-permeation chromatography (GPC) data also show that a decrease in average molecular weight occurs preferentially for the larger polymers after a long time

[1]Department of Chemistry, University of Illinois at Urbana-Champaign, Urbana, Illinois 61801, USA, [2]Beckman Institute for Advanced Science and Technology, University of Illinois at Urbana-Champaign, Urbana, Illinois 61801, USA, [3]Department of Aerospace Engineering, University of Illinois at Urbana-Champaign, Urbana, Illinois 61801, USA, [4]Department of Chemistry, University of Washington, Seattle, Washington 98195, USA, [5]Department of Chemistry and the PULSE Institute, Stanford University, Stanford, California 94305, USA, [6]SLAC National Accelerator Laboratory, Menlo Park, California 94025, USA; †Present address: Department of Chemical Engineering, Massachusetts Institute of Technology, Cambridge, Massachussetts 02139, USA. *e-mail: jsmoore@illinois.edu

Table 1 | Polymers used for initial study.

Polymer	M_n (kDa)	M_w (kDa)	PDI
PPA$_{26}^C$	16.5	25.6	1.6
PPA$_{90}^C$	58.2	89.6	1.5
PPA$_{458}^C$	254	458	1.8
PMA$_{103}^L$	86.4	103	1.2

Preparation of PPA: BF$_3$·OEt$_2$, CH$_2$Cl$_2$, −78 °C, 2 h (a); pyridine, −78 °C, 2 h (b). Polymer collected after precipitation into methanol and washing with methanol and diethyl ether. Polydispersity index (PDI) = M_w/M_n. Polymer name notation: C = cyclic, L = linear, no. = M_w. PMA$_{103}^L$ was prepared by single-electron transfer living radical polymerization[21]. Molecular weights were calculated by standard calibration with monodisperse polystyrene standards.

exposure to ultrasound. The residual macromolecules are chains from the original distribution, whose initial molecular weight was close to the mechanically activated threshold.

Because PPA is acid-sensitive, special care was taken to neutralize the solvent by stirring it with NaOH pellets (see Supplementary Section II for experimental details). As a control, PPA$_{26}^C$ was sonicated under the same conditions as PPA$_{90}^C$. If the reaction is caused by acid or heat, a time-dependent reduction in

molecular weight would also be expected for this polymer. If the change in M_w results from mechanical activation, the shorter polymer will retain its original molar mass, being too small to be force-activated. After 3 h of sonication, no significant change was observed for PPA$_{26}^C$ solutions, providing strong evidence that the depolymerization observed for PPA$_{90}^C$ is triggered by a mechanochemical process.

As a reference sample, PMA$_{103}^L$ with similar molecular weight to the PPA (Fig. 1c) was sonicated under the same conditions. As previously shown, the mean molecular weight for this polymer decreases, but the integrated intensity of the M_w distribution stays nearly constant[21]. Figure 1d compares the normalized change in the refractometer area with sonication time in each of the tested polymers. PPA$_{90}^C$ displays a clear decrease in area while the areas of the two controls remain unchanged, providing additional evidence that depolymerization to monomer is being triggered by mechanical force only for PPA$_{90}^C$.

Mechanistic study. For most polymers, mechanically induced chain scission results in a pair of macroradicals that terminate by atom abstraction or radical recombination[5]. PPA polymerization and depolymerization has been demonstrated through cationic and anionic mechanisms, but not by a radical mechanism, raising questions about the depolymerization mechanism. Unlike the prevalence of radical intermediates in typical mechanochemical reactions, heterolytic bond scission (which, in the case of PPA, would generate reactive hemiacetalate and oxocarbenium end groups) was shown to partially occur in solid-state mechanochemistry of polyolefins at 77 K in the presence of tetracyanoethylene[22–24]. Such reactivity was also proposed for the
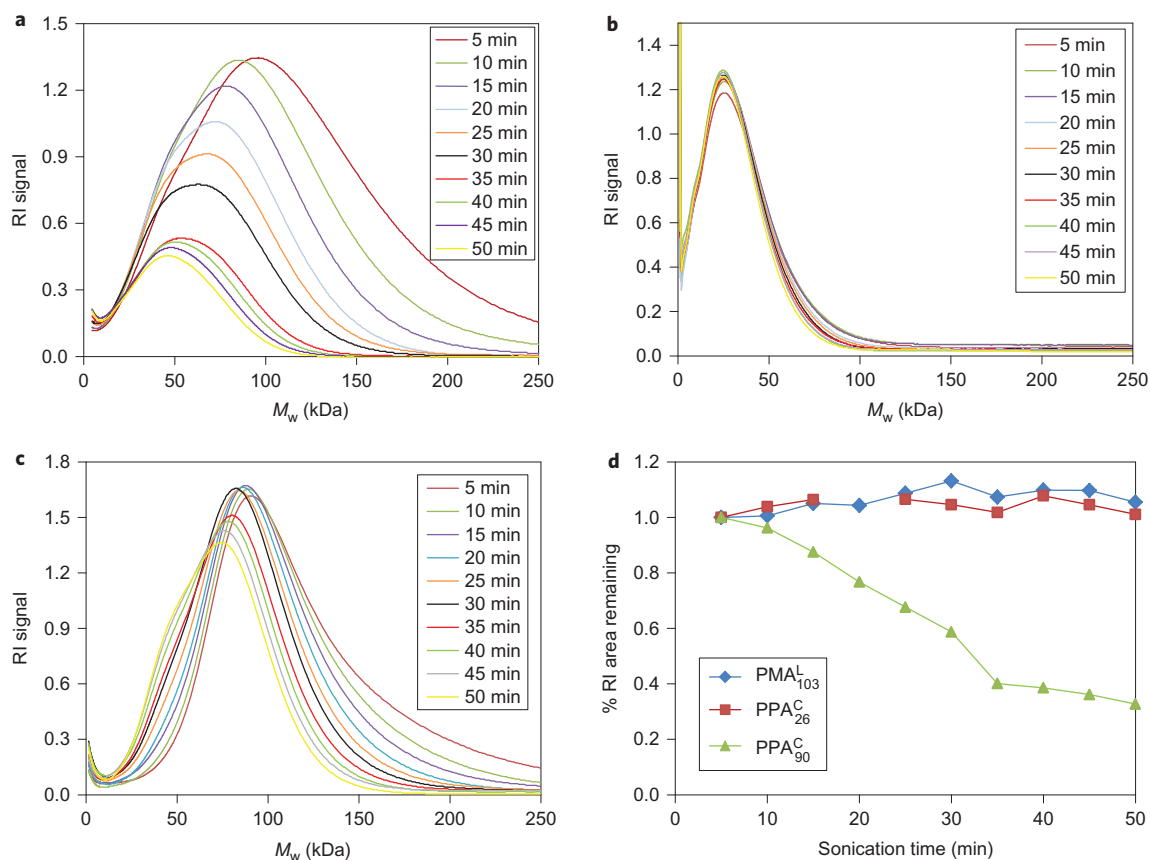
Figure 1 | GPC studies of sonicated polymers. a, PPA$_{90}^C$. **b**, PPA$_{26}^C$. **c**, PMA$_{103}^L$. **d**, Change in area ratio with sonication time for PPA$_{90}^C$, PPA$_{26}^C$ and PMA$_{103}^L$. RI, refractive index detector. Times indicate total 'on time' of pulsed ultrasound conducted at −15 °C, polymer concentration 1 mg ml^{-1} in THF, 8.7 W cm^{-2}. Final M_w values: 48.9 kDa (**a**), 23.6 kDa (**b**) and 65.0 kDa (**c**). The decrease in RI signal can only be observed for high-M_w PPA, indicating depolymerization is triggered only by mechanical force.
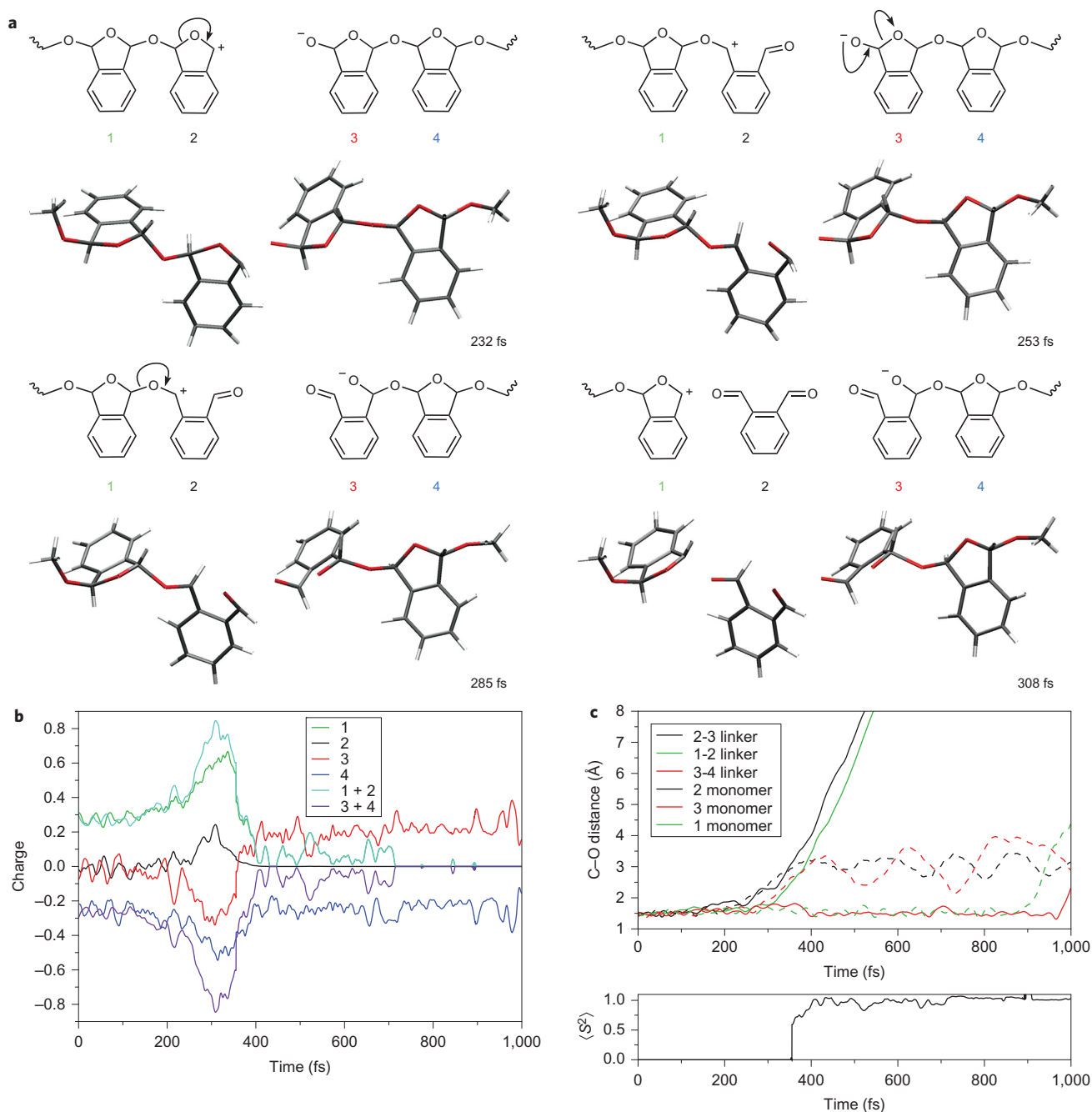
Figure 2 | Mechanistic studies by *ab initio* steered molecular dynamics calculations a, Snapshots with corresponding schematic reaction progress diagrams (showing numbering scheme for monomers). **b**, Charges on the numbered monomer fragments. **c**, Interatomic distances and expectation value of the electronic spin operator $\langle S^2 \rangle$ (see main text for details) for a representative molecular dynamics trajectory with steering force of 3.5 nN. The fragments remain charged throughout the initial bond cleavage and the first depolymerization propagation step, indicating heterolytic bond scission.

mechanochemical scission of poly(ethylene glycol) in water[25] and poly(dimethyl siloxane)[26].

To address the mechanistic question at hand, we carried out *ab initio* steered molecular dynamics calculations on the force-modified potential energy surface[27,28] using TeraChem[29]. The electronic structure was described with unrestricted density functional theory using the B3LYP exchange-correlation functional[30,31] and the 6-31G basis set[32]. Opposing steering forces were applied to the carbon atoms of the terminal methyl groups in a truncated model of the polymer with four monomer units. A total of ten simulations were followed for 1 ps under application of an external force of 3.5 nN, with initial conditions sampled from a 300 K finite-temperature Wigner distribution in the harmonic approximation.

Representative results from one simulation are displayed in Fig. 2. At this applied force, scission of one of the central linking C–O bonds occurs during the first ~230 fs. This first rupture is followed in rapid succession by subsequent opening of the five-membered rings of the inner PPA monomers and further dissociation of two monomers (labelled **1** and **2** in Fig. 2a). Analysis of the electronic density during the trajectory using Mulliken populations clearly indicates initial heterolytic cleavage (Fig. 2b) with charge separation persisting until after both linking bonds are broken. The lower panel of Fig. 2c shows that the wavefunction does not acquire any diradical character (radical character is indicated by a non-vanishing expectation value of the electronic spin operator $\langle S^2 \rangle$), which is approximately the number of spin-up electrons that

625
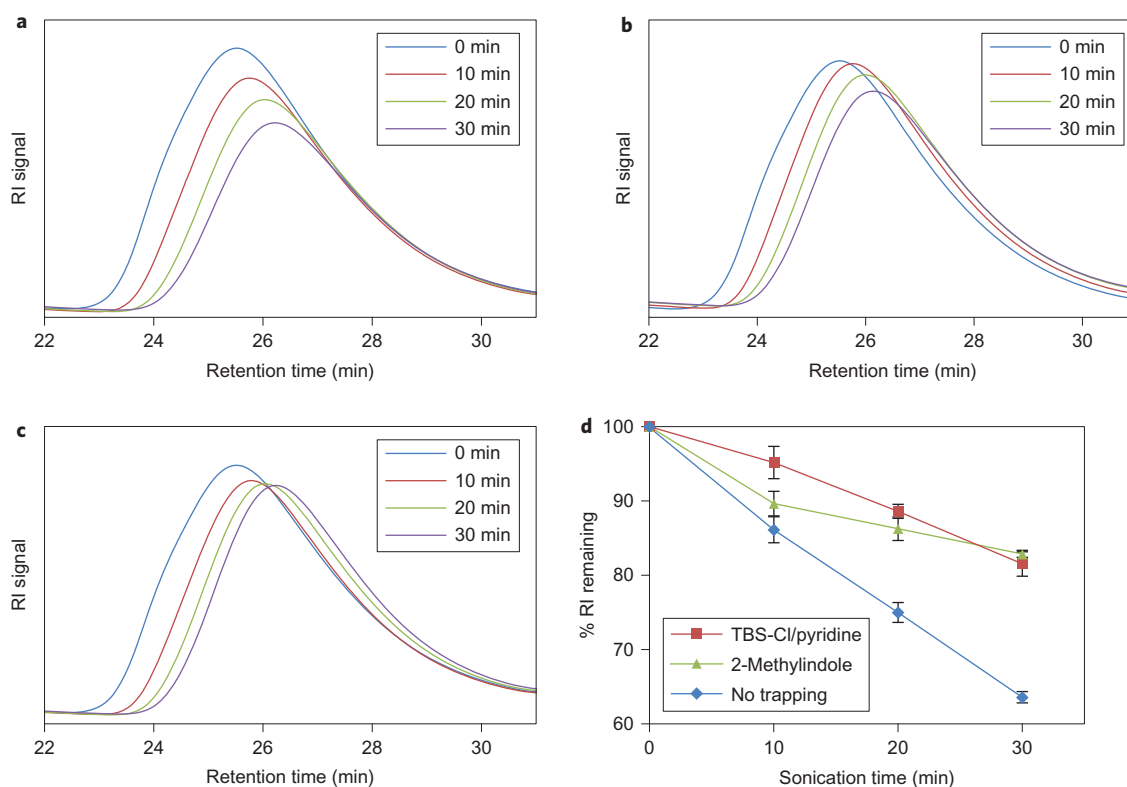
Figure 3 | GPC data for linear PPA$_{51}^L$ trapping experiments with increasing sonication time. a, No trapping agent. **b**, TBS-Cl and pyridine. **c**, 2-Methylindole. **d**, Plot of RI peak area versus sonication time (average of three runs; error bars represent standard deviations). Polymer solutions were prepared at 5 mg ml^{-1} and sonicated (13.7 W cm^{-2}) at 9 °C under N$_2$ atmosphere. Times indicate total 'on time' of ultrasound using a duty cycle of 1 s on, 9 s off. The RI is normalized to a 200 kDa polystyrene internal standard (3.0 mg ml^{-1}) added to the sample just before GPC injection. Final M_w values: 29.6 kDa (**a**), 37.0 kDa (**b**) and 31.6 kDa (**c**). Slowing depolymerization rates in the presence of the trapping reagents are consistent with a heterolytic bond scission mechanism.

are not paired with a spin-down counterpart) until after the initiation event has occurred. At an applied force of 3.5 nN, all ten steered molecular dynamics simulations lead to rupture of a linker bond followed by monomer rearrangement, as shown here. Similar results are also obtained at a lower applied force of 2.75 nN and using the larger 6-31G** basis set (see Supplementary Section V for discussion and results).

Trapping experiments. To experimentally verify the zwitterionic depolymerization, end group trapping experiments were conducted. Arresting the depolymerization of cyclic polymers is challenged by the need to simultaneously capture the hemiacetalate and oxocarbenium end groups. On the other hand, trapping either fragment of a linear polymer with a stable end cap will prevent the depolymerization of one half of the cleaved polymer, leading to a decrease in the rate of molecular weight reduction. Therefore, anionic polymerization[33] was used to prepare separate samples of linear PPA: PPA$_{51}^L$ ($M_w = 50.7$ kDa, polydispersity index (PDI) = 1.6) and PPA$_4^L$ (4.3 kDa, 1.2 PDI). PPA$_{51}^L$ was sonicated in THF without a trapping agent to provide baseline assessment of the breakdown rate (Fig. 3a). The observed degradation characteristics were consistent with those observed for cyclic PPA$_{90}^C$. To verify that the depolymerization of linear PPA$_{51}^L$ is exclusively mechanochemical, a low-molecular-weight control, PPA$_4^L$, was sonicated under the same conditions; no degradation was observed after 60 min of sonication time.

Sonication of the PPA$_{51}^L$ was then conducted separately in the presence of the electrophilic trapping agent TBS-Cl (Fig. 3b) and a nucleophilic trapping agent (2-methylindole, Fig. 3c) to trap either the hemiacetalate or oxocarbenium end groups, respectively.

In each case, production of lower-molecular-weight chains and a decrease in the rate of total polymer degradation (Fig. 3d) were observed, which are consistent with trapping of the chain ends. To experimentally explore the possibility of a homolytic cleavage mechanism, PPA$_{51}^L$ was also sonicated in the presence of a radical trap (TEMPO). No change in the rate of polymer degradation was observed, nor were there any signals in the NMR spectrum that would be consistent with incorporation of the TEMPO moiety. Additionally, no lower-molecular-weight fragments were observed. Collectively, these experiments support the heterolytic chain scission mechanism.

Polymer regeneration. Finally, to test the suitability of this system as a model of a regenerating system, depolymerization followed by repolymerization was pursued. The depolymerization product was identified after sonication of PPA$_{90}^C$ by precipitating and separating the residual polymer and concentrating the filtrate to dryness for analysis by gas chromatography mass spectrometry (GCMS). The gas chromatogram showed a single peak, which was identified as o-phthalaldehyde (OPA) by comparison to the mass spectrum of OPA in the NIST standard database. ^{1}H and ^{13}C NMR spectroscopy further confirmed OPA as the main product of the depolymerization, with clear aldehyde peaks both in ^{1}H and ^{13}C NMR (Supplementary Figs 3–7).

Because the ceiling temperature in OPA polymerization is concentration-dependent, we repeated the depolymerization at a concentration 100 times higher to enable effective repolymerization. Increasing the polymer concentration is known to decrease the rate of mechanochemical activation of polymers[5], so other parameters were changed to compensate and accelerate the reaction. Reaction
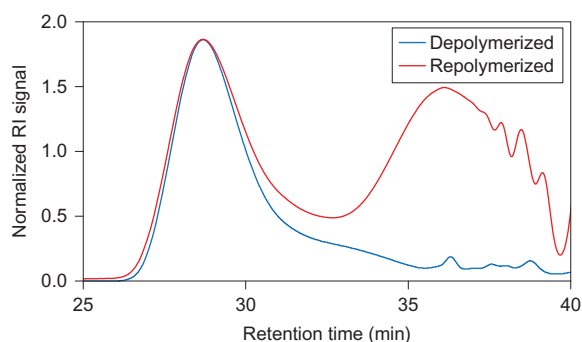
Figure 4 | Depolymerization–repolymerization of PPA in THF. GPC analysis of polymer solution after sonication (remaining polymer, blue; monomer peak not shown) and after repolymerization (red, remaining polymer + regenerated polymer). Final M_w values: depolymerized, 32.5 kDa; repolymerized, 32.5 and 1.9 kDa. Repolymerization produces new chains with different M_w, without affecting the remaining polymer.

rate increases with initial molecular weight and with decreasing temperature, so PPA_{458}^C was sonicated in THF at $-40\,^\circ$C (ref. 5). Under these conditions, sonication for 6 h resulted in ~60% depolymerization of the original polymer, as observed by GPC. As cationic polymerization is not possible in THF, we conducted anionic polymerization by cooling to $-78\,^\circ$C and adding n-BuLi as initiator. After 10 h, the polymer was end-capped by the addition of acetic anhydride and pyridine. The reaction solution was analysed by GPC, and two peaks were observed. One peak corresponded to the polymer remaining after sonication, while a new, lower-molecular-weight peak representing ~67% monomer recovery appeared (Fig. 4). The regenerated polymer has a different molecular weight from the initial chains, because the monomer/initiator ratio depends on the extent of depolymerization. However, glass-transition temperature (T_g) is fairly constant above a degree of polymerization (DP) of ~200 and brittle strength (flexural strength below T_g) over DP of ~600 (ref. 34). By using a small amount of initiator, repolymerization to DP > 600 can be achieved (Supplementary Fig. 10). Importantly, the repolymerization occurred with no effect on the remaining polymer.

Conclusions

We have demonstrated the mechanochemically triggered depolymerization of high-M_w linear and cyclic PPA. Low-molecular-weight PPA does not undergo significant depolymerization under similar conditions, supporting the proposed mechanical triggering mechanism. *Ab initio* steered molecular dynamics calculations pointed towards a heterolytic scission mechanism, atypical for mechanochemical bond scission. We propose that, in the case of cyclic PPA, bond scission produces a linear zwitterionic chain containing oxocarbenium and hemiacetalate chain ends, both of which undergo head-to-tail depolymerization above T_c to produce OPA monomer. Linear PPA, on the other hand, produces two half chains, one terminated by an oxocarbenium and one by an hemiacetalate, each of which undergoes rapid depolymerization. This mechanism was supported experimentally by trapping the oxocarbenium with a nucleophilic reagent, and the hemiacetalate with an electrophile, causing not only a reduction of the depolymerization rate, but also the appearance of lower-molecular-weight chains that were not observed in the absence of the trapping reagents. Furthermore, depolymerization produced OPA monomer, which was successfully repolymerized to PPA using an anionic initiator, successfully completing a depolymerization–repolymerization cycle. These essential steps point towards the development of functional materials where aging or mechanical damage initiates depolymerization of the polymer chains back to

monomers, which are then available for repolymerization to heal damage or remodel the materials system. Work towards developing new metastable polymers with higher ceiling temperatures is under way, which will enable the development of remodelling materials for room-temperature applications.

References
1. Berg, J. M., Tymoczko, J. L. & Stryer, L. *Biochemistry* (W. H. Freeman, 2010).
2. Wu, G. Amino acids: metabolism, functions, and nutrition. *Amino Acids* **37**, 1–17 (2009).
3. Sinnot, M. *Carbohydrate Chemistry and Biochemistry: Structure and Mechanism* (Royal Society of Chemistry, 2012).
4. Blackburn, G. M., Gait, M. J., Loakes, D. & Williams, D. *Nucleic Acids in Chemistry and Biology* (Royal Society of Chemistry, 2006).
5. Caruso, M. M. *et al.* Mechanically-induced chemical changes in polymeric materials. *Chem. Rev.* **109**, 5755–5798 (2009).
6. May, P. A. & Moore, J. S. Polymer mechanochemistry: techniques to generate molecular force via elongational flows. *Chem. Soc. Rev.* **42**, 7497–7506 (2013).
7. Peterson, G. I., Larsen, M. B. & Boydston, A. J. Controlled depolymerization: stimuli-responsive self-immolative polymers. *Macromolecules* **45**, 7317–7328 (2012).
8. Wang, W. & Alexander, C. Self-immolative polymers. *Angew. Chem. Int. Ed.* **47**, 7804–7806 (2008).
9. Sagi, A., Weinstain, R., Karton, N. & Shabat, D. Self-immolative polymers. *J. Am. Chem. Soc.* **130**, 5434–5435 (2008).
10. Teitelbaum, S. L. Bone resorption by osteoclasts. *Science* **289**, 1504–1508 (2000).
11. Fratzl, P., Gupta, H. S., Paschalis, E. P. & Roschger, P. Structure and mechanical quality of the collagen–mineral nanocomposite in bone. *J. Mater. Chem.* **14**, 2115–2123 (2004).
12. Eriksen, E. F. Normal and pathological remodeling of human trabecular bone: 3-dimensional reconstruction of the remodeling sequence in normals and in metabolic bone-disease. *Endocrin. Rev.* **7**, 379–408 (1986).
13. Parfitt, A. M. Osteonal and hemi-osteonal remodeling: the spatial and temporal framework for signal traffic in adult human bone. *J. Cell Biochem.* **55**, 273–286 (1994).
14. Aso, C., Tagami, S. & Kunitake, T. Polymerization of aromatic aldehydes. II. Cationic cyclopolymerization of phthalaldehyde. *J. Polym. Sci. A* **7**, 497–511 (1969).
15. Tsuda, M., Hata, M., Nishida, R. & Oikawa, S. Acid-catalyzed degradation mechanism of poly(phthalaldehyde): unzipping reaction of chemical amplification resist. *J. Polym. Sci. A* **35**, 77–89 (1997).
16. Nguyen, T. Q., Liang, Q. Z. & Kausch, H-H. Kinetics of ultrasonic and transient elongational flow degradation: a comparative study. *Polymer* **38**, 3783–3793 (1997).
17. Craig, S. L. Mechanochemistry: a tour of force. *Nature* **487**, 176–177 (2012).
18. Wiggins, K. M., Brantley, J. N. & Bielawski, C. W. Polymer mechanochemistry: force enabled transformations. *ACS Macro Lett.* **1**, 623–626 (2012).
19. Kaitz, J. A., Diesendruck, C. E. & Moore, J. S. End group characterization of poly(phthalaldehyde): surprising discovery of a reversible, cationic macrocyclization mechanism. *J. Am. Chem. Soc.* **135**, 12755–12761 (2013).
20. Rosen, B. M. & Percec, V. Single-electron transfer and single-electron transfer degenerative chain transfer living radical polymerization. *Chem. Rev.* **109**, 5069–5119 (2009).
21. Kryger, M. J. *et al.* Masked cyanoacrylates unveiled by mechanical force. *J. Am. Chem. Soc.* **132**, 4558–4559 (2010).
22. Sakaguchi, M. *et al.* Ionic species produced by mechanical fracture of solid polymer. III. Anions from polytetrafluoroethylene. *J. Polym. Sci. B* **25**, 1431–1437 (1987).
23. Sakaguchi, M. *et al.* Ionic products from the mechanical fracture of solid polypropylene. *Polymer* **25**, 944–946 (1984).
24. Sakaguchi, M., Makino, M., Ohura, T. & Iwata, T. Mechanoanions produced by mechanical fracture of bacterial cellulose: ionic nature of glycosidic linkage and electrostatic charging. *J. Phys. Chem. A* **116**, 9872–9877 (2012).
25. Aktah, D. & Frank, I. Breaking bonds by mechanical stress: when do electrons decide for the other side? *J. Am. Chem. Soc.* **124**, 3402–3406 (2002).
26. Thomas, J. R. & deVries, L. Sonically induced heterolytic cleavage of polymethylsiloxane. *J. Phys. Chem.* **63**, 253–256 (1959).
27. Ong, M. T. *et al.* First principles dynamics and minimum energy pathways for mechanochemical ring opening of cyclobutene. *J. Am. Chem. Soc.* **131**, 6377–6379 (2009).
28. Israelwitz, B., Gao, M. & Schulten, K. Steered molecular dynamics and mechanical function of proteins. *Curr. Opin. Struct. Biol.* **11**, 224–230 (2001).
29. Ufimtsev, I. S. & Martinez, T. J. Quantum chemistry on graphical processing units. 3. Analytical energy gradients, geometry optimization, and first principles molecular dynamics. *J. Chem. Theor. Comp.* **5**, 2619–2628 (2009).

30. Becke, A. D. Density functional thermochemistry. III. The role of exact exchange. *J. Chem. Phys.* **98,** 5648–5652 (1993).

31. Lee, C., Yang, W. & Parr, R. G. Development of the Colle–Salvetti correlation-energy formula into a functional of the electron density. *Phys. Rev. B* **37,** 785–789 (1988).

32. Hehre, W. J. R., Ditchfield, R. & Pople, J. A. Self-consistent molecular orbital methods. XII. Further extensions of Gaussian-type basis sets for use in molecular orbital studies of organic molecules. *J. Chem. Phys.* **56,** 2257–2261 (1972).

33. DiLauro, A., Robbins, J. S. & Phillips, S. T. Reproducible and scalable synthesis of end-cap-functionalized depolymerizable poly(phthalaldehydes). *Macromolecules* **46,** 2963–2968 (2013).

34. Seitz, J. T. The estimation of mechanical properties of polymers from molecular structure. *J. Appl. Polym. Sci.* **49,** 1331–1351 (1993).

Acknowledgements

Author contributions

J.S.M., T.J.M., A.J.B. and S.R.W. directed the research. J.S.M., A.J.B., C.E.D. and P.A.M. conceived the idea. C.E.D., G.I.P., J.A.K. and P.A.M. performed the experiments. H.J.K. and B.D.M. conducted the theoretical studies. All authors participated in writing the manuscript.

Additional information

Supplementary information is available in the online version of the paper. Reprints and permissions information is available online at www.nature.com/reprints. Correspondence and requests for materials should be addressed to J.S.M.

Competing financial interests

The authors declare no competing financial interests.